

Steven V. Vasiloff*
NOAA/National Severe Storms Laboratory, Norman, Oklahoma

1. INTRODUCTION

The National Weather Service (NWS) Weather Surveillance Radar - 1988 Doppler (WSR-88D) default reflectivity-rain rate (Z-R) relation is $Z=300R^{1.4}$ in the Precipitation Processing System (PPS; Fulton et al. 1998). The default Z-R relation typically works best with convective rainfall. Recently, the National Weather Service Radar Operations Center (NWS ROC) has recommended additional Z-R relations to improve precipitation estimates for non-convective storms; $Z=75R^2$ is recommended for "winter stratiform precipitation west of the continental divide" (ROC 1999).

Although a wider variety of Z-R relations is now available to forecasters, new procedures are needed for a real-time Z-R adjustment since a fixed Z-R is subject to error due to the large variations in precipitation processes within and among storms (e.g., Fujiyoshi et al. 1990). These variations depend on many factors including the particle density, fall speed, and the refractive indices for ice and water. Rasmussen et al. (2001) recognized this in the development of the Weather Support to Deicing Decision Making System (WSDDM) that uses real-time snow gauge data to adjust radar precipitation estimates during real-time sampling. The WSDDM system integrates gauge data and radar precipitation estimates and computes a new Z-R coefficient every radar volume based on the ratio of the two integrated quantities.

Increasing radar beam width and height with increasing range from the radar results in a decorrelation between the radar and gauge estimates with increasing range. At some point, the beam will entirely over-shoot the top of the storm. Several studies have documented efforts to compensate for range effects. Seo et al. (2000) proposed a real-time adjustment of radar range biases using a vertical profile of reflectivity (VPR). Joss and Lee (1995) derived range correction factors based on climatological VPRs in mountainous terrain. While these range corrections may improve radar QPE, it is believed that a robust real-time gauge adjustment will eliminate the need for this extra processing.

Another significant challenge to accurate precipitation estimates in mountainous terrain is the

* Corresponding author's address: Steve Vasiloff, NWS, WR Hq, 125 S. State Street Room 1210, SLC, UT 84138; e-mail: steven.vasiloff@noaa.gov

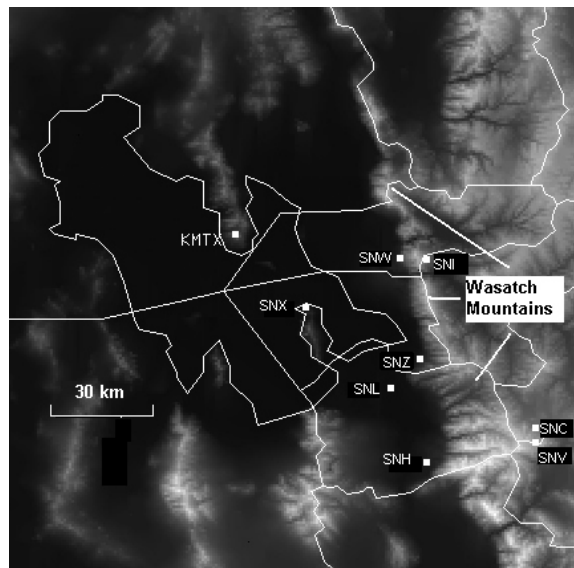


Figure 1. Topographic image of the Great Salt Lake and Wasatch mountains in northern Utah. The KMTX WSR-88D and Snetnet sites are also shown.

actual coverage which is reduced by beam blockage for radars located in valleys and by poor low-altitude coverage for radars sited on mountain tops. The height of effective coverage depends on the type of weather. For example, in a study of WSR-88D coverage along the West coast, Westrick et al. (1999) showed that the Medford, Oregon WSR-88D has a 0.5 km effective coverage range based on the average cool season melting level. Their analysis assumed that the maximum height of useful coverage is below the melting level or radar "bright band," a band of exaggerated radar returns caused by melting ice. Since the average melting level height was near the height of the radar, the lowest sweep scanned, on average, very little space below the bright band. In a study of WSR-88D coverage at on average, very little space below the bright band. In a study different heights (both MSL and AGL) for the conterminous U.S., Maddox et al. (2001) show that there is almost no coverage below 1 km AGL in the West.

Until new procedures are built into the radar system, forecasters need a way to evaluate, at least qualitatively, the accuracy of their radar precipitation estimates. This paper explores the accuracy of winter-time WSR-88D precipitation estimates in the mountainous area of northern Utah. This is the first study to document the performance of the WSR-88D during snow events in the western U.S. Snow water

Table 1. Range, width and height (AGL) of 0.5 deg beam at Snownet sites. The radar is ~2 km above sea level. *Height is for 1.4 deg elevation angle.

	SNI	SNW	SNX	SNZ	SNL	SNH	SNC	SNV
Range (km)	50	43	31	65	68	93	103	107
Beam width (km)	.8	.7	.5	1.0	1.1	1.5	1.7	1.8
Beam center height (km)	1.1*	1.0	1.2	1.3	1.5	1.9	1.4	1.1

Table 2. Number and type of events at Snownet sites.

	SNI	SNW	SNX	SNZ	SNL	SNH	SNC	SNV	MTN	VAL
Snow	42	3	2	18	16	14	34	24	100	53
Rain	0	3	7	14	14	11	0	0	0	49
Mix	2	5	2	12	12	7	1	0	103	38
Total	44	11	11	44	42	32	35	24	103	140

equivalent (SWE) estimates were derived with the relation $Z=75S^2$. Hereafter the variable "S" is used in place of "R," both having units of mm h^{-1} , since the focus is on snowfall. Correction factors were calculated from linear regression analyses based on a special network of snow gauges (called "Snownet") deployed at various ranges and altitudes from the WSR-88D in the complex terrain. A similar approach was used by Creutin et al. (1997). The correction factors are then related to the width of the radar beam, the height of the beam center above the area of interest, and the precipitation type. The correction factors are surrogates for an optimized Z-S. Since forecasters have a limited choice of Z-S relations, it is felt that at least a qualitative adjustment would be an operational improvement.

The ROC will soon incorporate a new Snow Accumulation Algorithm (SAA) into the WSR-88D system. Precipitation estimates used in this study were derived from the implementation of the SAA in the WSR-88D Algorithm Testing and Display System (WATADS; NSSL 1998). This study provides an early assessment of the SAA performance in complex terrain.

2. BACKGROUND

2.1 Topography

Figure 1 shows the study area and its topography. The KMTX WSR-88D is located on Promontory Point at the top of the Promontory Mountains that rise 700 m above the Great Salt Lake (GSL). This location provides coverage to the maximum range of 230 km (mainly for tall thunderstorms) at the expense of low-altitude coverage over the populated valleys of northern Utah, especially along the western edge of the Wasatch Mountains. For

example, Vasiloff (2001) showed that the 0.5 deg beam height of ~1500 m over Salt Lake City (SLC) resulted in the radar's failure to detect the formation of an upward-developing tornado that moved through downtown SLC. Other low-altitude phenomena that are undetected include lake breezes and thunderstorm outflow winds.

Table 1 lists KMTX beam characteristics over the Snownet sites. SNX is on Antelope Island in the GSL and even at the close range of 31 km, the beam is relatively high at 1.2 km AGL. In contrast, SNV, located next to a ski run at Deer Valley Resort, is at a range of 107 km with the beam center at 1.1 km AGL. However, the beam width at SNV is nearly 2.5 times wider than at SNX. SNI is located mid-mountain at Snowbasin Ski Area and is in an area of blockage at the 0.5 deg sweep. Thus, the height of the beam is computed from the 1.4 deg sweep. SNC is the third mountain site and is located near the base of the Park City Mountain Resort. The remaining sites are considered valley sites with the possible exception of SNW which is at the base of the west side of Mount Ogden. SNH is the most distant valley site at 93 km range. The beam is fairly high there as well, nearly 2 km AGL. Finally, SNL, at the Salt Lake International airport behind the SLC Weather Forecast Office, is at a range similar to the Bountiful site (SNZ) although SNZ is closer to the mountains.

2.2 Gauge measurements

SWE estimates used in this study were made by ETI and GEONOR snow gauges. These gauges were described in detail by Rasmussen et al. (2001). The gauges both use antifreeze to melt snowfall and a weighing mechanism determines the increase in the liquid's weight which is, in turn, converted to a depth. The ETI uses a pressure transducer to measure weight and has a depth resolution of .01" (.25 mm). The

GEONOR gauges use a vibrating wire to measure the weight change and has an advertised depth resolution of .001" (.025 mm). All Snownet sites had ETI gauges with single Alter shields during the winter of 1998/99. In the winter of 1999/00, ETI gauges at SNL, SNZ, SNH, and SNC were replaced with GEONOR gauges. Tests of these gauges with various types of shields were conducted at the National Center for Atmospheric Research's Marshall test site (Rasmussen et al. 1999 and Rasmussen et al. 2001). Test results show that measurements using the ETI and GEONOR with a Wyoming shield were nearly identical to manual measurements. Table 2 lists the number and type of event for each Snownet site. An event is listed as all rain if the temperature at the site was 3 C or greater and all snow if the temperature was 0 C or less. Data between 0 C and 3 C are considered mixed events. Indeed, mountain snow/valley rain is a common occurrence in the West. It is important to separate the rain and snow events because the dielectric constant, particle density and fall speed are different for water and ice and affect the coefficient in the Z-S relation. Only 2 gauges, SNI and SNZ, recorded all 44 events. SNW and SNX had frequent communication and equipment outages and recorded only 11 events. Communication problems also hampered data collection at SNH and SNV. Another reason for fewer recorded events is that some sites may not have had any precipitation. There was a combined total of 103 mountain and 140 valley events.

2.3 Radar estimates

As mentioned above, radar SWE estimates were derived using the new SAA. This algorithm was initially made available in NSSL's WATADS and will be implemented in the WSR-88D radar products generator. The SAA is very similar to the current PPS and differs primarily in the way ground clutter/anomalous propagation are rejected and precipitation post-processing (e.g., the PPS bias adjustment which is not used in the SAA). While the default SAA Z-S relation is $Z=150S^2$, this study employed the relation $Z=75S^2$ since it is currently recommended for operational use. One-hour SWE accumulations directly over the gauge sites were recorded. Surrounding radar bins were sampled to ensure that ground clutter values were not recorded.

A simple overhead measurement is subject to error from both vertical and horizontal gradients of reflectivity. Several instances were observed whereby precipitation over a site was not measured by the gauge. In some cases, the lack of measured precipitation was the result of horizontal advection. In other cases, the low-altitudes were relatively dry resulting in sublimation. These problems result in scatter of the data and will be discussed more later.

3. RESULTS

For each site, a gauge estimate is matched

with a radar estimate, i.e., a number of radar-gauge (R-G) pairs are generated. A scatter plot of 1-hr estimates for SNI is shown in Fig. 2. There are 307 hourly estimates with a correlation of .70 and a large amount of scatter. The conclusion from this figure is that there is huge variance between the radar and gauge estimates. Some of the variance can be explained by natural variance in the Z-S relation and some can be explained by radar sampling artifacts such as the difference between sampling volumes and horizontal advection. Multi-hour accumulations from the same data set are shown in Fig. 3a. There is a much better correspondence between the radar and gauge: much less scatter with a correlation of .88. Thus, the use of multi-hour totals reduces errors caused by timing and spatial discrepancies as well as potential gauge catch inefficiencies. The benefit of longer accumulation time periods in associating radar and gauge data has been shown by others to reduce uncertainties (e.g., Rosenfeld 1998 and Fujiiyoshi et al. 1990). Thus, the remainder of this paper will be restricted to "storm total" accumulations.

Figures 3b-h shows storm-total R-G scatter plots for remaining sites. The correlations, a measure of the scatter about the linear fit (with $R = 1$ indicating a perfect relationship), are all fairly high except for SNW and SNX, whose low values may be the result of the small data samples.

As mentioned above, the coefficient in the Z-S relation is dependent on precipitation type. Since the data base contains snow, rain, and snow-rain mix cases (see Table 2), the data were subdivided to test for relationships between regression results and

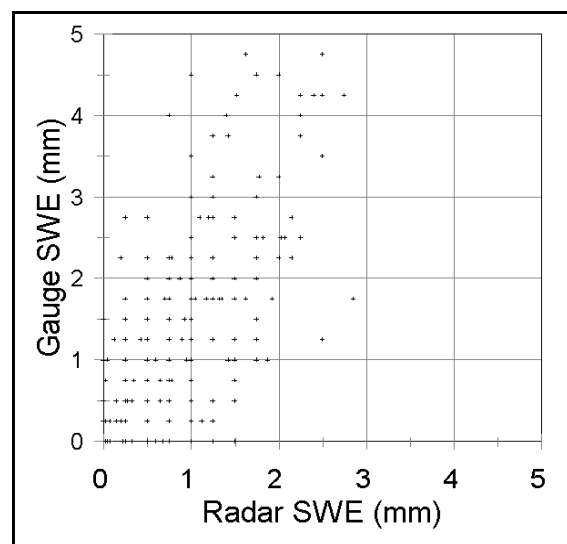


Figure 2. Scatter plot of radar vs. gauge 1-hour SWE amounts for Snowbasin (SNI).

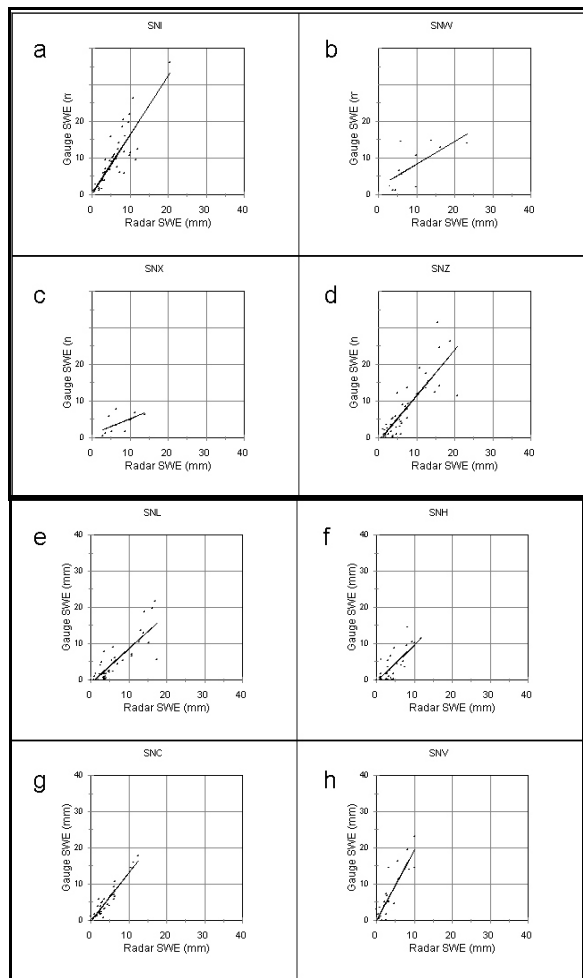


Figure 3. As in Fig. 2 except for storm total amounts at a) SNI, b) SNW, c) SNX, d) SNZ, e) SNL, f) SNH, g) SNC, and h) SNV.

precipitation type. Figure 4 shows the CF for each valley site for rain and snow as well as two groups of mixed precipitation. Mountain sites are not plotted since they had few rain or mixed events. Sites SNX and SNW were omitted because of the small data sample. "Mix1" is all rain cases combined with the mixed precipitation cases. "Mix2" is all snow cases combined with the mixed precipitation cases. Because of the possibility that the 0 C and 3 C cutoffs may not be exact (e.g., there may be all snow cases having temperatures less than 3 C) it is thought that adding the Mix1 and Mix2 groups might help identify any trends overlooked by the otherwise course grouping. Indeed, there is a distinctive trend of lower CFs with decreasing temperature. Notably, the CF's converge to a value close to 0.75 indicating that the radar is underestimating precipitation during snow events.

The ratio of normalized beam width to normalized beam height (W/H quotient) was computed and related to the CF's (Fig. 5). There is a much better

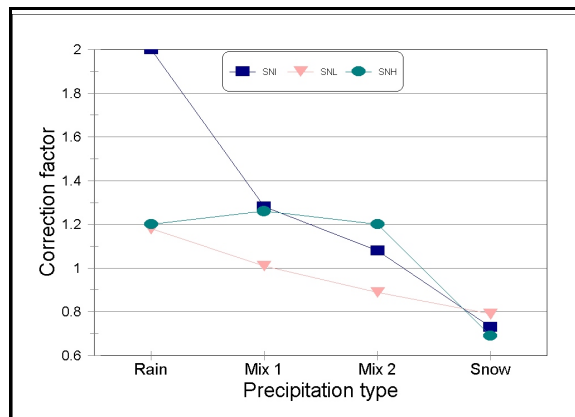


Figure 4. Correction factors for SNZ, SNL, and SNH for different precipitation types.

relationship between the W/H quotient and CF than there is between the CF and either the beam width or height individually, namely that the CF increases with increasing quotient. SNI is somewhat of an outlier; possibly related to local precipitation processes in that area. Differentiating CF by altitude, i.e., mountain versus valley locations, leads to a similar conclusion. Scatter plots for all-mountain, all-valley, and snow-only valley cases are shown in Fig. 6. The CF for all-mountain cases is 1.63 (radar is under-estimating) with a correlation of .87. The CF for all-valley sites is 1.01 (radar is nearly perfect) and the correlation is .90. For valley snow only cases, the CF is .75 (radar is over-estimating) with a correlation of .83. Indexing CF to other parameters, such as storm type, may shed further light on the nature of the CF with respect to location; however, that is beyond the scope of this paper. The CF's derived here are analogous to a range adjustment where upward adjustments are made to radar estimates

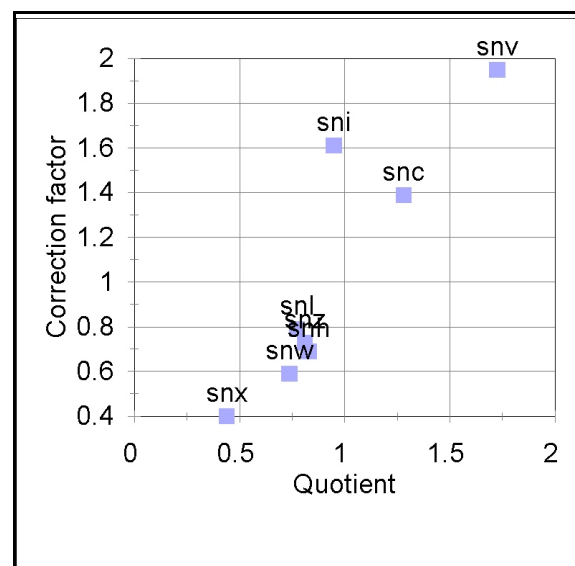


Figure 5. Correction factors as a function of the ratio of beam height and width for each Snownet site.

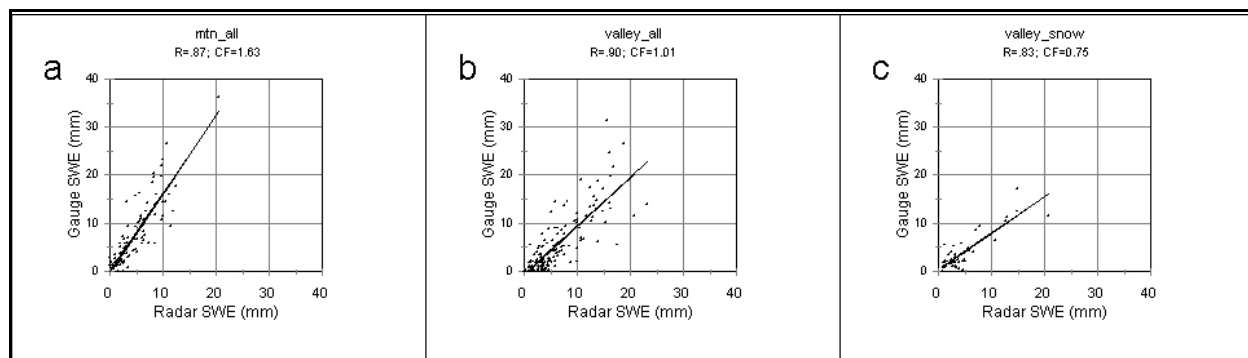


Figure 6. As in Fig. 2 except for a) all mountain observations, b) all valley observations, and c) all valley snow observations. Correlation coefficients (R) and correction factors (CF) are shown for each plot.

at far ranges and downward adjustments are made at near ranges, as discussed in Seo et al. (2000). Creutin et al. (1997) also reported upward adjustments for rainfall estimates at farther ranges. However, adjustments described here cannot be quantitatively compared to adjustments made in Seo et al. and Creutin et al. since their data sets consisted of all surface rainfall while the radar typically sampled ice aloft.

4. CONCLUSIONS

Precipitation estimates from the KMTX WSR-88D at Promontory Point in northern Utah were compared to snow gauge data for 44 winter storms. The $Z-S$ relation $Z=75S^2$ was used to derive snow water equivalent precipitation rate from the reflectivity data. It was found that a static $Z-S$ is inadequate for hourly snowfall estimates and that correlations between the radar and gauges improved for longer time averages. Thus, real-time radar calibration is needed using calibrated snow gauges. In the absence of a real-time correction, results from this study could be used to make gross corrections for at least the point locations where gauge data were compared to radar estimates. In general, for all-snow cases, the radar underestimated precipitation in the Wasatch Mountains and overestimated precipitation at the valley locations just west of the Wasatch. Correction factors for adjusting the radar estimates were 1.63 and 0.75 for mountain and valley locations, respectively. Because of the complicated relationships between the radar beam characteristics and the terrain, errors as a function of only range could not be identified. Instead, there appeared to be a distinct relationship between the ratio of the beam width to beam center height above the gauge with smaller ratios having smaller correction factors. Since the farthest valley gauge from the radar was 97 km, these results are limited to relatively close ranges since the radar samples out to 230 km range. However, because the KMTX radar is located on a mountain, it is not expected that the radar will adequately sample shallow winter storms, especially in

mountain valleys, much beyond the ranges discussed in this study. On the other hand, distant peaks may be associated with reasonable radar estimates but only after further study into range effects.

These results indicate that the new SAA will be an overall improvement to WSR-88D wintertime precipitation estimates in complex terrain. The primary benefit will be through the added flexibility of changing the $Z-R/S$ relation depending on the situation. After the SAA is installed, it is recommended that the relation $Z=75S^2$ be used everywhere with additional corrections previously described for mountains and valleys within ~100 km of the radar. Also, the hybrid scan files need fine-tuning for areas of beam blockage. In this study, a minimum in storm-total estimates was discovered along the 134 deg azimuth. The minimum was caused by beam blockage close to the radar. The ROC should be notified whenever such discrepancies between radar precipitation estimates and hybrid scan files are observed. These discrepancies can be most easily identified through comparison of the hybrid scan images and storm-total precipitation fields.

5. ACKNOWLEDGMENTS

The author thanks J.J. Gourley, Dr. Robert A. Maddox, and Dr. Roy Rasmussen for their reviews and helpful suggestions that improved this manuscript. Special appreciation is expressed to Drs. Maddox and Rasmussen who provided invaluable guidance during the course of data gathering and analysis.

6. REFERENCES

- Creutin, J. D., H. Andrieu, and D. Faure, 1997: Use of a weather radar for the hydrology of a mountainous area. Part II: radar measurement validation. *J. Hydro.*, **193**, 26-44.
- Fulton, R. A., J. P. Breidenbach, D.-J. Seo, D. A. Miller, and T. O'Bannon, 1998: The WSR-88D rainfall algorithm. *Wea. Forecasting*, **13**, 388-395.

- Fujiyoshi, Y., T. Endoh, T. Yamada, K. Tsuboki, Y. Tachibana, and G. Wakahama, 1990: Determination of a Z-R relationship for snowfall using a radar and high sensitivity snow gauges. *J. App. Meteor.*, **29**, 147-152.
- Joss, J., and R. Lee, 1995: the application of radar-gauge comparisons to operational precipitation profile corrections. *J. App. Meteor.*, **34**, 2612-2630.
- Maddox, R. A., J. Zhang, J. J. Gourley, and J. W. Howard, 2001: WSR-88D radar coverage over the coterminous United States. Submitted to *J. Wea. Forecasting*.
- O'Bannon, T., 1997: Using a 'terrain-based' hybrid scan to improve WSR-88D precipitation estimates. Preprints, *28th Conf. on Radar Meteorology*, Austin, TX, Amer. Meteor. Soc., 506-507.
- Rasmussen, R. M., J. Vivekanandan, J. Cole, B. Myers, and C. Masters, 1999: The estimation of snowfall rate using visibility. *J. App. Meteor.*, **38**, 1542-1563.
- _____, M. Dixon, F. Hage, J. Cole, C. Wade, J. Tuttle, S. McGettigan, T. Carty, L. Steveson, W. Fellner, S. Knight, E. Karplus, and N. Rehak, 2001: Weather Support to Deicing Decision Making System (WSDDM): A winter weather nowcasting system. *Bull. Amer. Meteor. Soc.*, **82**, 579-595.
- Radar Operations Center (formerly the Operational Support Facility) memorandum, December 15, 1999: Recommended changes to improve WSR-88D precipitation estimates during cool season stratiform rain events.
- Rosenfeld, D., and E. Amitai, 1998: Comparison of WPMM versus regression for evaluating Z-R relations. *J. App. Meteor.*, **37**, 1241-1249.
- Seo, D.-J., J. Breidenbach, R. Fulton, and D. Miller, 2000: Real-time adjustment of range-dependent biases in WSR-88D rainfall estimates due to nonuniform vertical profile of reflectivity. *J. Hydromet.*, **1**, 222-240.
- Vasiloff, S. V., 2001: Improving tornado warnings with the Federal Aviation Administration's Terminal Doppler Weather Radar. *Bull. Amer. Meteor. Soc.*, **82**, 861-874.
- WATADS (WSR-88D Algorithm Testing and Display System) 2000: Reference Guide for Version 10.2 [Available from Storm Scale Applications Division, National Severe Storms Laboratory, 1313 Halley Circle, Norman, OK 73069.]
- Westrick, K. J, C. F. Mass, and B. A. Colle, 1999: The limitations of the WSR-88D radar network for quantitative precipitation measurements over the coastal western United States. *Bull. Amer. Meteor. Soc.*, **80**, 2289-2298.